



HAL
open science

Complex resonance frequencies of a finite, circular radiating duct with an infinite flange

Bastien Mallaroni, Pierre-Olivier Mattei, Jean Kergomard

► **To cite this version:**

Bastien Mallaroni, Pierre-Olivier Mattei, Jean Kergomard. Complex resonance frequencies of a finite, circular radiating duct with an infinite flange. 2009. hal-00402870v1

HAL Id: hal-00402870

<https://hal.science/hal-00402870v1>

Preprint submitted on 10 Jul 2009 (v1), last revised 11 Jan 2010 (v2)

HAL is a multi-disciplinary open access archive for the deposit and dissemination of scientific research documents, whether they are published or not. The documents may come from teaching and research institutions in France or abroad, or from public or private research centers.

L'archive ouverte pluridisciplinaire **HAL**, est destinée au dépôt et à la diffusion de documents scientifiques de niveau recherche, publiés ou non, émanant des établissements d'enseignement et de recherche français ou étrangers, des laboratoires publics ou privés.

**Complex resonance frequencies of a finite, circular radiating duct with an
infinite flange**

Bastien Mallaroni,^{a)} Pierre-Olivier Mattei, and Jean Kergomard

Laboratoire de Mécanique et d'Acoustique

31 chemin Joseph Aiguier

13402 Marseille Cedex 20 (France)

(Dated: July 10, 2009)

Abstract

The pressure field inside a flanged duct of finite length radiating on one side in an infinite medium can be described from the knowledge of a radiation matrix impedance, as proposed by Zorumski. In order to calculate the resonance frequencies (which are complex because of the energy loss by radiation), the formulation used in Zorumski's theory must be modified as it is not valid for complex frequencies. The analytical development of the Green's function in free space used by Zorumski depends on the integrals of Bessel functions which become divergent for complex frequencies. This paper purposes a development of the Green's function which is valid for all frequencies. The results are applied to the calculation of the complex resonance frequencies of a flanged duct of finite length, by using a formulation of the internal pressure based upon cascade impedance matrices. It presents and discusses the influence of higher order duct modes and the results for several duct radius/length ratios.

PACS numbers: 43.20.Rz, 43.20.Mv

I. INTRODUCTION

Green's functions are widely used in many physical situations and notably in acoustics, for the calculation of the pressure field radiated by physical sources (*e.g.* speakers, musical instruments, vibrating structures,...). For instance, the solution given by Rayleigh¹ to the classical problem of a plane piston radiating into an infinite flange involves the Green's function in free space. Zorumski² extended this result to obtain the radiation of a semi-infinite flanged duct in the form of matrix impedance, giving the coupling between duct modes and used the Sonine's infinite integral (Ref. 3, p.416, Eq.4) to develop the Green's function in free space. In Refs 4, 5, formulations based on the Zorumski's method of this radiation impedance are obtained for a larger class of problems. However, the development fails when the frequency becomes complex: the corresponding infinite integral, involving a Bessel function whose argument is a product of the frequency and the dummy argument, becomes divergent for complex frequencies. In many studies, the Zorumski's radiation matrix is used as a boundary condition at the end of the duct in order to calculate input impedances, length corrections or reflection coefficients (see *e.g.* Refs. 6 or 7). To the authors' knowledge, no studies have been reported on the calculation of modes inside the duct for the problem of a duct with an infinite flange. The modes are complex and have complex resonance frequencies (in the literature, the modes are called either eigenmodes or resonance modes, and must be distinguished from the duct modes used in the present paper for the purpose of the calculation). It is worth noting that complex resonance frequencies can occur in various situations (*e.g.* dissipative fluid, radiation, complex impedance wall boundary conditions such as in Refs. 8 or 9). In section II of this paper, we present a new expression for the Green's function in free space for complex frequencies. In section IV, an application of this result is devoted to the determination of the complex resonance frequencies of a cylindrical duct, closed at its input, considering the influence of higher order duct modes and several radius/length ratios. For this purpose, the internal Green's function is previously calculated

^{a)}Electronic address: mallaroni@lma.cnrs-mrs.fr

in section III with a method of cascade impedance.

II. CALCULATIONS OF GREEN'S FUNCTION FOR THE HELMHOLTZ EQUATION IN FREE SPACE

Many studies on sound radiation by cylindrical ducts can be found in the literature. For the case of an infinite flange, Norris and Sheng¹⁰ or Nomura¹¹ used a Green's function integral to find an appropriate formulation for the external field. We can also cite the classical work by Levine and Schwinger¹² for the case of an unflanged pipe. Zorumski² extended the results for the planar mode to obtain a multimodal radiation impedance which is a combination of the duct modes present in the duct. In this section, these calculations are briefly recalled, exhibiting the difficulty related to complex frequencies. Thus, a new analytical formula for the Green's function, valid for a dissipative problem, is presented.

A. Zorumski's radiation impedance

We consider the radiation of sound into an infinite half space from a circular duct (with radius b and length L), with an infinite flange at $z_0 = 0$ (the index 0 corresponds to the cross section S_0 at the end of the duct) and we have chosen to work with circular coordinates where the vector \mathbf{r} is denoted (z, r, θ) as shown by Fig. 1.

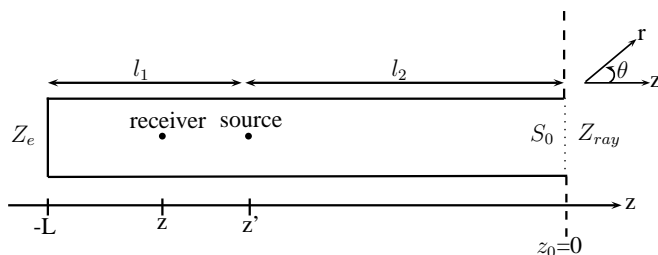


FIG. 1. Schema and coordinates of the duct.

The acoustic pressure in the infinite medium ($z \geq 0$) is given by a Helmholtz integral

(the time factor $\exp(-i\omega t)$ is omitted throughout this paper):

$$p(\mathbf{r}) = -\frac{i\omega\rho}{2\pi} \int_0^{2\pi} \int_0^b r_0 v(r_0, \theta_0) \frac{e^{ikh}}{h} dr_0 d\theta_0, \quad (1)$$

where $h = [r^2 + r_0^2 - 2rr_0 \cos(\theta - \theta_0) + z^2]^{\frac{1}{2}}$, ρ the ambient density and the wavenumber $k = \omega/c$ (with ω the circular frequency and c the speed of sound).

The pressure p and the velocity v inside the duct ($z < 0$) are expressed as a series of duct eigen modes, so in $z = 0$:

$$p(r, \theta, z = 0) = \rho c^2 \sum_m \sum_n \psi_{mn}(kr) e^{im\theta} P_{mn}, \quad (2)$$

$$v(r, \theta, z = 0) = c \sum_m \sum_n \psi_{mn}(kr) e^{im\theta} V_{mn}, \quad (3)$$

where $\psi_{mn}(kr)e^{im\theta}$ is the transverse function for the mode mn with $\psi_{mn}(kr) = J_0(kr)/N_{mn}$. The λ_{mn} are the eigenvalues, solutions of $J'(\lambda_{mn}kb) = 0$, and the norm N_{mn} is chosen similarly to that used by Zorumski².

Substituting Eq. (3) into Eq. (1) gives the pressure for $z \geq 0$ in terms of the modal velocity amplitudes V_{mn} :

$$p(r, \theta, z) = -\frac{i\omega\rho c}{2\pi} \sum_m \sum_n V_{mn} \int_0^{2\pi} e^{im\theta_0} \int_0^b r_0 \frac{e^{ikh}}{h} \psi_{mn}(kr_0) dr_0 d\theta_0. \quad (4)$$

Zorumski expressed the free space Green's function in equation (4) in terms of a Sonine's infinite integral (3, p. 416, Eq. 4) and wrote for $z = 0$ in the expression of h :

$$\frac{e^{ikh}}{h} = k \int_0^\infty \tau(\tau^2 - 1)^{-\frac{1}{2}} J_0(\tau kh) d\tau. \quad (5)$$

Next, he introduced a concept of "generalized radiation impedance matrix \mathbf{Z}_{ray} " for a semi-infinite duct with an infinite flange to describe the relation between the modal pressure and velocity amplitudes:

$$P_{mn} = \sum_{l=1}^{\infty} Z_{mnl} V_{ml}, \quad (6)$$

where m , l and n are, respectively, the orders of circumferential, radial incident and reflected modes. The element Z_{mnl} of the radiation impedance matrix gives the contribution of the velocity mode ml to the pressure mode mn (for reasons of symmetry, the coupling is possible

only for a duct mode with the same azimuthal dependence). The expression of the radiation impedance is obtained as:

$$Z_{mnl} = -i \int_0^\infty \tau(\tau^2 - 1)^{-\frac{1}{2}} D_{mn}(\tau, k) D_{ml}(\tau, k) d\tau, \quad (7)$$

with, for a hard wall condition:

$$D_{mn}(\tau, k) = kb \frac{\tau \psi_{mn}(kb) J'_m(\tau kb)}{\lambda_{mn}^2 - \tau^2}. \quad (8)$$

B. Green's function for the Helmholtz equation in free space for complex frequencies

The following asymptotic form (see Ref. 13, Eq. 9.2.1, p. 364) occurs when ν is fixed and $|\kappa| \rightarrow \infty$:

$$J_\nu(\kappa) = \sqrt{\frac{2}{\pi\kappa}} \left[\cos\left(\kappa - \frac{1}{2}\nu\pi - \frac{1}{4}\pi\right) + e^{|\Im(\kappa)|} O(|\kappa|^{-1}) \right], \quad (9)$$

with $|\arg \kappa| < \pi$ (in this paper, the real part and imaginary part are represented, respectively, by the symbols \Re and \Im). As a consequence, for $\tau \rightarrow \infty$ with $k \in \mathbb{C}$ we have $J_0(\tau kh) \rightarrow \infty$ when $\Im(k) \neq 0$, thus relation (5) and the radiation impedance (7) given by Zorumski are divergent integrals for all non real frequencies.

In order to have a Green's function for the Helmholtz equation in free space valid for complex frequencies, we use another form of the Sonine's infinite integral to develop this Green's function, expressed by Watson³ (p. 416, Eq. 4):

$$\frac{e^{ikh}}{h} = \int_0^\infty \tau(\tau^2 - k^2)^{-\frac{1}{2}} J_0(\tau h) d\tau. \quad (10)$$

This integral remains convergent even for k complex. A difficulty occurs since k is a branch point of the square root. For a time factor $\exp(-i\omega t)$, the integration path on the real axis must remain below k . However the complex resonance frequencies $\omega = ck$ have a negative imaginary part (see explanation in section IV), so the previous formula must be adapted because of the branch cut. The integration path below k is classically deformed, as shown in Fig. 2:

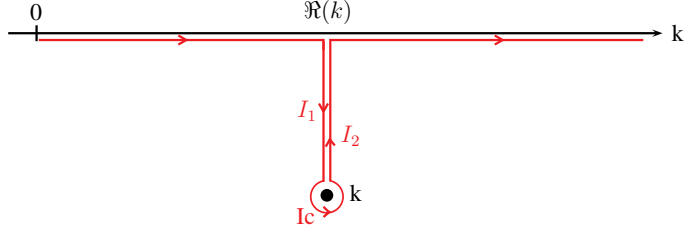


FIG. 2. Deformation of the integration contour.

Now, the integral in Eq. (10) is written as:

$$\frac{e^{ikh}}{h} = \int_0^{|\Re(k)|} J_0(\tau h) \tau (\tau^2 - k^2)^{-\frac{1}{2}} d\tau + I_1(k, h) + I_c + I_2(k, h) + \int_{|\Re(k)|}^{\infty} J_0(\tau h) \tau (\tau^2 - k^2)^{-\frac{1}{2}} d\tau, \quad (11)$$

with

$$I_1(k, h) = I_2(k, h) = - \int_{|\Re(k)|}^k J_0(\tau h) \tau (\tau^2 - k^2)^{-\frac{1}{2}} d\tau$$

and I_c is zero according to Jordan's lemma.

After calculations (similar to those developed by Morse and Feshbach¹⁴, p.410), the following five cases can be distinguished:

i) $\Re(k) \leq 0$ and $\Im(k) > 0$

$$\frac{e^{ikh}}{h} = \int_0^{\infty} J_0(\tau h) \tau (\tau^2 - k^2)^{-\frac{1}{2}} d\tau. \quad (12)$$

ii) $\Re(k) \leq 0$ and $\Im(k) \leq 0$

$$\begin{aligned} \frac{e^{ikh}}{h} = & -i \int_0^{|\Re(k)|} J_0(\tau h) \frac{\tau}{\sqrt{k^2 - \tau^2}} d\tau + \int_{|\Re(k)|}^{\infty} J_0(\tau h) \frac{\tau}{\sqrt{\tau^2 - k^2}} d\tau \\ & - 2 \int_{|\Re(k)|}^k J_0(\tau h) \frac{\tau}{\sqrt{\tau^2 - k^2}} d\tau. \end{aligned} \quad (13)$$

iii) $\Re(k) > 0$ and $\Im(k) > 0$

$$\frac{e^{ikh}}{h} = +i \int_0^{|\Re(k)|} J_0(\tau h) \frac{\tau}{\sqrt{k^2 - \tau^2}} d\tau + \int_{|\Re(k)|}^{\infty} J_0(\tau h) \frac{\tau}{\sqrt{\tau^2 - k^2}} d\tau. \quad (14)$$

iv) $\Re(k) > 0$ and $\Im(k) = 0$

$$\begin{aligned} \frac{e^{ikh}}{h} &= J_0(kh)k\sqrt{2\epsilon}(1-i) + i \int_0^{|k|(1-\epsilon)} J_0(\tau h) \frac{\tau}{\sqrt{k^2 - \tau^2}} d\tau \\ &+ \int_{|k|(1+\epsilon)}^{\infty} J_0(\tau h) \frac{\tau}{\sqrt{\tau^2 - k^2}} d\tau, \end{aligned} \quad (15)$$

with $\epsilon \ll 1$.

v) $\Re(k) > 0$ and $\Im(k) < 0$

$$\begin{aligned} \frac{e^{ikh}}{h} &= +i \int_0^{|\Re(k)|} J_0(\tau h) \frac{\tau}{\sqrt{k^2 - \tau^2}} d\tau + \int_{|\Re(k)|}^{\infty} J_0(\tau h) \frac{\tau}{\sqrt{\tau^2 - k^2}} d\tau \\ &- 2 \int_{|\Re(k)|}^k J_0(\tau h) \frac{\tau}{\sqrt{\tau^2 - k^2}} d\tau. \end{aligned} \quad (16)$$

Contrary to the original Zorumski's formulation, these results involve convergent integrals when the frequency is complex.

C. New formulation of generalized impedance of a flanged circular duct for real frequencies

Initially, the previous result will be checked for the real case, in order to compare the original Zorumski's result, noted in Eq. (7), and that obtained using the expansion of $\exp(ikh)/h$ for the case (iv) where $\Im(k) = 0$. Eq. (15) leads to the following results:

$$\begin{aligned} Z_{mnl} &= -ik[\tilde{D}_{mn}(k)\tilde{D}_{ml}(k)k\sqrt{2\epsilon}(1-i) + i \int_0^{|k|(1-\epsilon)} \frac{\tau}{\sqrt{k^2 - \tau^2}} \tilde{D}_{mn}(\tau)\tilde{D}_{ml}(\tau) d\tau \\ &+ \int_{|k|(1+\epsilon)}^{\infty} \frac{\tau}{\sqrt{\tau^2 - k^2}} \tilde{D}_{mn}(\tau)\tilde{D}_{ml}(\tau) d\tau], \end{aligned} \quad (17)$$

where

$$\tilde{D}_{mn}(\tau) = b \frac{\tau \psi_{mn}(b) J'_m(\tau b)}{\lambda_{mn}^2 - \tau^2}. \quad (18)$$

Figure 3 shows the comparison of the radiation impedance for the planar mode ($m = n = 0$ with $l = 0$) with Zorumski's formulation (7) and formulation (17) (with $\epsilon = 10^{-6}$). This confirms the validity of formula (17) with the identical computational cost. This formula is used in Ref. 15 to calculate an approximation of the reflection coefficient and of the

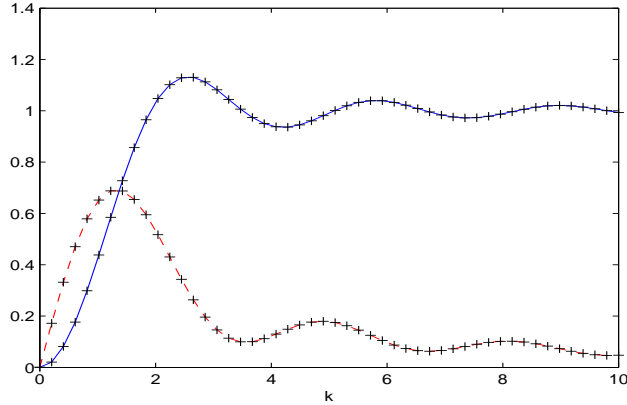


FIG. 3. Real part (solid curve) and absolute value of imaginary part (dashed curve) of the radiation impedance for the planar mode ($m = n = 0$ and $l = 0$) with respect to wavenumber k , calculated with Zorumski's formulation (7) (solid and dashed curves) and with modified formulation (17) (crosses).

length correction, taking into account the effect of the higher order duct modes below the first cut-off frequency.

The comparison between complex Zorumski's formulation for the planar mode ($m=n=0$ and $l=0$) and Rayleigh's radiation impedance of a flanged plane piston confirm the validity of Z_{000} for all the frequencies (see Appendix C), because Rayleigh's radiation impedance is by definition the same quantity as Z_{000} .

In what follows, we show the interest of the radiation impedance valid for complex frequencies when calculating the complex resonance frequencies of a flanged finite length duct terminating in a Zorumski's radiation condition. In a first instance, the internal Green's function must be determined, with a method of cascade impedances.

III. CALCULATION OF THE FINITE FLANGED DUCT INTERNAL GREEN'S FUNCTION WITH A METHOD OF CASCADE IMPEDANCES

A. Definition of the internal Green's function

We search for the internal Green's function $G(M, M', \omega)$ at a point $M(r, \theta, z)$ with a source in $M'(r', \theta', z')$, satisfying:

$$(\Delta_M + k^2)G(M, M', \omega) = -\frac{1}{2\pi r}\delta(r - r')\delta(\theta - \theta')\delta(z - z'), \quad (19)$$

with $\partial_n G(M, M', \omega) = 0$ on the walls. It is classically (see e.g. Morse and Feshbach¹⁴) expanded in a series of duct modes (the boundary conditions for the variable z will be given later on):

$$G(M, M', \omega) = \sum_{m=0}^{\infty} \sum_{n=0}^{\infty} \phi_{mn}(r, \theta) \phi_{mn}(r', \theta') g_{mn}(z, z', \omega), \quad (20)$$

where $\phi_{mn}(r, \theta) = \psi_{mn}(r)e^{im\theta}$ is the transverse function for the mode mn and $g_{mn}(z, z', \omega)$ is the longitudinal function for the mode mn . In what follows, the dependance in ω of $g_{mn}(z, z', \omega)$ is omitted for simplicity. It is worth noting that now we have the transverse function with respect to r and not kr , as per Zorumski². Therefore, $\psi_{mn}(r) = \frac{J_m(\lambda_{mn}r)}{N_{mn}}$ where the λ_{mn} are solutions of $J'_m(\lambda_{mn}b) = 0$, with $\lambda_{mn} = \gamma_{mn}/b$. The γ_{mn} are the $(n+1)^{th}$ zeros of the first derivative of the Bessel's function J_m . The following norm N_{mn} is chosen (Ref. 2):

$$N_{mn} = b\sqrt{\pi} \sqrt{1 - \frac{m^2}{\lambda_{mn}^2 b^2}} J_m(\lambda_{mn}b). \quad (21)$$

The transverse modes $\phi_{mn}(r, \theta)$ satisfy:

$$(\Delta_{\perp} + \lambda_{mn}^2)\phi_{mn}(r, \theta) = 0,$$

with $\Delta_{\perp} = \frac{1}{r}\frac{\partial}{\partial r}(r\frac{\partial}{\partial r}) + \frac{1}{r^2}\frac{\partial^2}{\partial \theta^2}$, thus: $\Delta_{\perp}\phi_{mn}(r, \theta) = -\lambda_{mn}^2\phi_{mn}(r, \theta)$. Studies such as Refs. 6 or 7 show that a small finite number of terms is necessary for a numerical estimate of the summation and it can be truncated: M_m is defined as the number of circumferential modes m and N_n as the number of radial modes n . Introducing the previous expression (20) in

(19) gives:

$$\sum_{m=0}^{M_m} \sum_{n=0}^{N_n} \left(\frac{\partial^2}{\partial z^2} + k_{mn}^2 \right) \phi_{mn}(r, \theta) \phi_{mn}(r', \theta') g_{mn}(z, z') = -\frac{1}{2\pi r} \delta(r - r') \delta(\theta - \theta') \delta(z - z'), \quad (22)$$

where $k_{mn}^2 = k^2 - \lambda_{mn}^2$. Then, multiplying the left and right sides of (22) by $\phi_{m'l}^*(r, \theta)$ and integrating the resulting equality on the surface S, the orthogonality condition ($\int_S \phi_{mn} \phi_{m'l}^* dS = \delta_{mm'} \delta_{nl}$), leads to:

$$\left(\frac{\partial^2}{\partial z^2} + k_{mn}^2 \right) g_{mn}(z, z') = -\delta(z - z'). \quad (23)$$

With a conservative Neumann or Dirichlet boundary condition at the extremities of the duct, the resonance wavenumbers can be easily computed. But with a dissipative boundary condition like those occurring for the sound radiation of a flanged cylinder, there is no simple analytical solution. Therefore, in the next section, the elements $g_{mn}(z, z')$ are calculated with a method of cascade impedances presented in Refs. 6,16 or 17.

B. Presentation of the method of cascade impedances

The calculation of the duct impedance at an abscissa z_1 with respect to another abscissa z_2 is based on the following transfer matrix relationship (see e.g. Ref. 17):

$$\begin{pmatrix} P_{mn}(z_1) \\ V_{mn}(z_1) \end{pmatrix} = (M_T) \begin{pmatrix} P_{mn}(z_2) \\ V_{mn}(z_2) \end{pmatrix}, \quad (24)$$

$M_T = \begin{pmatrix} \cosh(ik_{mn}(z_2 - z_1)) & Z_{c,mn} \sinh(ik_{mn}(z_2 - z_1)) \\ \frac{\sinh(ik_{mn}(z_2 - z_1))}{Z_{c,mn}} & \cosh(ik_{mn}(z_2 - z_1)) \end{pmatrix}$, where $Z_{c,mn}$ is an element of the diagonal matrix of characteristic impedance \mathbf{Z}_c :

$$Z_{c,mn} = \frac{k\rho c}{k_{mn}}.$$

Moreover, matrices formulation is chosen: $\Phi(r, \theta)$ is a column vector constituted by the $M_m N_n$ elements ϕ_{mn} , verifying $\int_S \Phi(r, \theta) \Phi^T(r, \theta) dS = \mathbf{I}$, $\mathbf{P}(z)$ is a column vector constituted by the $M_m N_n$ elements P_{mn} and $\mathbf{V}(z)$ is a column vector constituted by the $M_m N_n$ elements

V_{mn} . Thus, relation (24) is now written:

$$\begin{pmatrix} \mathbf{P}(z_1) \\ \mathbf{V}(z_1) \end{pmatrix} = \begin{pmatrix} \mathbf{C} & \mathbf{Z}_c \mathbf{S} \\ \mathbf{Z}_c^{-1} \mathbf{S} & \mathbf{C} \end{pmatrix} \begin{pmatrix} \mathbf{P}(z_2) \\ \mathbf{V}(z_2) \end{pmatrix}, \quad (25)$$

where \mathbf{C} and \mathbf{S} are diagonal matrices constituted by the elements $\cosh(ik_{mn}(z_2 - z_1))$ and $\sinh(ik_{mn}(z_2 - z_1))$, respectively.

The transfer matrix formulation (25) is now transformed into an impedance matrix formulation. The calculation, presented in Ref. 17, is recalled in Appendix A. This gives the following matrix equation:

$$\begin{pmatrix} \mathbf{P}(z_1) \\ \mathbf{P}(z_2) \end{pmatrix} = \begin{pmatrix} \mathbf{Z}_{11} & -\mathbf{Z}_{12} \\ \mathbf{Z}_{21} & -\mathbf{Z}_{22} \end{pmatrix} \begin{pmatrix} \mathbf{V}(z_1) \\ \mathbf{V}(z_2) \end{pmatrix}, \quad (26)$$

where $\mathbf{Z}_{11} = \mathbf{Z}_c \mathbf{S}^{-1} \mathbf{C}$, $\mathbf{Z}_{12} = \mathbf{Z}_c \mathbf{S}^{-1}$, $\mathbf{Z}_{21} = \mathbf{Z}_c \mathbf{S}^{-1}$ and $\mathbf{Z}_{22} = \mathbf{Z}_c \mathbf{S}^{-1} \mathbf{C}$.

C. Calculation of $\mathbf{P}(z')$

First, the pressure vector at the source position z' is calculated. For this purpose, we calculate a right-side matrix impedance $\mathbf{Z}^+(z')$ at z' with respect to \mathbf{Z}_{ray} , a left-side matrix impedance $\mathbf{Z}^-(z')$ at z' with respect to \mathbf{Z}_e and finally the connection between these two matrices at z' , the abscissa of the source.

Step 1: Right-side matrix impedance $\mathbf{Z}^+(z')$

Let us denote \mathbf{C}_s and \mathbf{S}_s the diagonal matrix constituted by the elements $\cosh(ik_{mn}l_2)$ and $\sinh(ik_{mn}l_2)$, respectively, where l_2 (see Fig. 1) is the distance between the abscissa z' and the extremity ($z = 0$). The radiation impedance \mathbf{Z}_{ray} , constituted by the elements Z_{mnl} calculated in the previous section, verifies $\mathbf{P}(z' + l_2) = \mathbf{Z}_{\text{ray}} \mathbf{V}(z' + l_2)$. Thus Eq. (25) leads to:

$$\mathbf{V}(z' + l_2) = (\mathbf{Z}_{\text{ray}} + \mathbf{Z}_{22})^{-1} \mathbf{Z}_{21} \mathbf{V}(z'), \quad (27)$$

and, with Eqs. (26) and (27), to:

$$\mathbf{P}(z') = \mathbf{Z}_{11} \mathbf{V}(z') - \mathbf{Z}_{12} (\mathbf{Z}_{\text{ray}} + \mathbf{Z}_{22})^{-1} \mathbf{Z}_{21} \mathbf{V}(z').$$

With \mathbf{Z}^+ verifying $\mathbf{P}(z') = \mathbf{Z}^+(z')\mathbf{V}(z')$, we have finally:

$$\mathbf{Z}^+(z') = \mathbf{Z}_{11} - \mathbf{Z}_{12}(\mathbf{Z}_{\text{ray}} + \mathbf{Z}_{22})^{-1}\mathbf{Z}_{21}, \quad (28)$$

or:

$$\mathbf{Z}^+(z') = \mathbf{Z}_c \mathbf{S}_s^{-1} \mathbf{C}_s - \mathbf{Z}_c \mathbf{S}_s^{-1} [\mathbf{Z}_c^{-1} \mathbf{Z}_{\text{ray}} + \mathbf{S}_s^{-1} \mathbf{C}_s]^{-1} \mathbf{S}_s^{-1}. \quad (29)$$

Step 2: Left-side matrix impedance $\mathbf{Z}^-(z')$

We choose a Neumann condition for $z = -L$ (thus $\mathbf{V}(z' - l_1) = 0$). Here, \mathbf{C}_e and \mathbf{S}_e are the diagonal matrices constituted by the elements $\cosh(ik_{mn}l_1)$ and $\sinh(ik_{mn}l_1)$, respectively. l_1 (see Fig. 1) is the distance between the point $z = -L$ and the point z' . The impedance \mathbf{Z}_e is calculated at $z = -L$.

Relation (26) is written for the present case as:

$$\mathbf{P}(z') = \mathbf{Z}_c \mathbf{S}_e^{-1} \mathbf{V}(z' - l_1) - \mathbf{Z}_c \mathbf{S}_e^{-1} \mathbf{C}_e \mathbf{V}(z'). \quad (30)$$

Thus, with the Neumann condition in $z = -L$ and with Eq. (30), using $\mathbf{P}(z') = \mathbf{Z}^-(z')\mathbf{V}(z')$, the following result is obtained:

$$\mathbf{Z}^-(z') = -\mathbf{Z}_c \mathbf{S}_e^{-1} \mathbf{C}_e. \quad (31)$$

Step 3: Connection between the impedance matrices \mathbf{Z}^+ and \mathbf{Z}^- at z'

Let us denote $P_{mn}^\pm(z') = [g_{mn}(z, z')]_{z=z' \pm \epsilon}$. Using the continuity of the Green's function at $z = z'$, leads to when $\epsilon \rightarrow 0$:

$$P_{mn}^+(z') = P_{mn}^-(z') = P_{mn}(z'), \quad (32)$$

Integrating relation (23) on an interval of width 2ϵ between $z' + \epsilon$ and $z' - \epsilon$ gives:

$$\int_{z'-\epsilon}^{z'+\epsilon} \left(\frac{\partial^2}{\partial z^2} + k_{mn}^2 \right) g_{mn}(z, z') dz = -1 \quad (33)$$

and, with the pressure continuity, when $\epsilon \rightarrow 0$:

$$\partial_z P_{mn}^+(z') - \partial_z P_{mn}^-(z') = -1, \quad (34)$$

with $\partial_z P_{mn}^\pm(z') = [\partial_z g_{mn}(z, z')]_{z=z' \pm \epsilon}$.

Euler's equation $\frac{1}{\rho c} V_{mn}(z') = -\frac{1}{i\omega\rho} \partial_z P_{mn}(z')$ implies $\partial_z P_{mn}(z') = -ikV_{mn}(z')$, thus, using Eq. (34):

$$V_{mn}^+(z') - V_{mn}^-(z') = \frac{1}{ik}. \quad (35)$$

We introduce a column vector \mathbf{W} of $M_m N_n$ lines whose elements equal 1. Equation (35) may be expressed as:

$$(\mathbf{Z}^+(z'))^{-1} \mathbf{P}^+(z') - (\mathbf{Z}^-(z'))^{-1} \mathbf{P}^-(z') = \frac{1}{ik} \mathbf{W},$$

and using Eq. (32), the pressure at the source is written as follows:

$$\mathbf{P}(z') = \frac{1}{ik} [(\mathbf{Z}^+(z'))^{-1} - (\mathbf{Z}^-(z'))^{-1}]^{-1} \mathbf{W}. \quad (36)$$

D. Expression of the function $\mathbf{g}(z, z')$

We introduce a column vector $\mathbf{g}(z, z')$ constituted by the $M_m N_n$ elements $g_{mn}(z, z')$. They are two possible configurations with respect to the relative positions of receiver at z and source at z' :

First configuration: $z > z'$

Let $l_r = z - z'$ be the distance between the receiver and the source (see Fig. 1), $\mathbf{C}_{\mathbf{l}_r}$ the diagonal matrix constituted by the elements $\cosh(ik_{mn}l_r)$, and $\mathbf{S}_{\mathbf{l}_r}$ the diagonal matrix constituted by the elements $\sinh(ik_{mn}l_r)$. Relation (24) gives for $z > z'$:

$$\mathbf{g}(z, z') = \mathbf{C}_{\mathbf{l}_r} \mathbf{P}(z') - \mathbf{Z}_c \mathbf{S}_{\mathbf{l}_r} \mathbf{V}(z'),$$

then, with $\mathbf{P}(z') = \mathbf{Z}^+(z') \mathbf{V}(z')$:

$$\mathbf{g}(z, z') = \mathbf{S}_{\mathbf{l}_r} [\mathbf{S}_{\mathbf{l}_r}^{-1} \mathbf{C}_{\mathbf{l}_r} - \mathbf{Z}_c (\mathbf{Z}^+(z'))^{-1}] \mathbf{P}(z'). \quad (37)$$

Second configuration: $z' > z$

Let $l_l = z' - z$ be the distance between the receiver and the source (see Fig. 1), $\mathbf{C}_{\mathbf{l}_l}$ the diagonal matrix constituted by the elements $\cosh(ik_{mn}l_l)$, and $\mathbf{S}_{\mathbf{l}_l}$ the diagonal matrix constituted

by the elements $\sinh(ik_{mn}l)$. Relation (24) gives for $z' > z$:

$$\mathbf{g}(z, z') = \mathbf{C}_1 \mathbf{P}(z') + \mathbf{Z}_c \mathbf{S}_1 \mathbf{V}(z'),$$

then, with $\mathbf{P}(z') = \mathbf{Z}^-(z') \mathbf{V}(z')$:

$$\mathbf{g}(z, z') = \mathbf{S}_1 [\mathbf{S}_1^{-1} \mathbf{C}_1 + \mathbf{Z}_c (\mathbf{Z}^-(z'))^{-1}] \mathbf{P}(z'). \quad (38)$$

Finally, the Green's function of a finite duct with an infinite flange is given as:

$$\mathbf{G}(M, M') = \mathbf{\Phi}(r, \theta) \mathbf{\Phi}(r', \theta') \mathbf{g}(z, z'). \quad (39)$$

IV. APPLICATION TO COMPLEX RESONANCE FREQUENCIES OF A FLANGED, FINITE LENGTH DUCT

Resonances of a flanged, finite length duct are interesting as they contain important information about the coupling between internal and external fluids. Their calculation is based on the fact that the internal pressure becomes infinite at each resonance. Newton's method is used to compute the zeros of the inverse of the pressure. Since the resonances of a dissipative problem are complex, a complex formulation of the impedance radiation is needed. As a time dependence $\exp(-i\omega t)$ has been chosen, the imaginary part needs to be negative for resonance frequencies in order to ensure that the amplitude remains bounded for all times t . Using the integrals (13) and (16), for $\Re(k) > 0$ and $\Im(k) < 0$, Z_{mnl} becomes:

$$\begin{aligned} Z_{mnl} = & -ik \left[i \int_0^{|\Re(k)|} \frac{\tau}{\sqrt{k^2 - \tau^2}} \tilde{D}_{mn}(\tau) \tilde{D}_{ml}(\tau) d\tau + \int_{|\Re(k)|}^{+\infty} \frac{\tau}{\sqrt{\tau^2 - k^2}} \tilde{D}_{mn}(\tau) \tilde{D}_{ml}(\tau) d\tau \right. \\ & \left. - 2 \int_{|\Re(k)|}^k \frac{\tau}{\sqrt{\tau^2 - k^2}} \tilde{D}_{mn}(\tau) \tilde{D}_{ml}(\tau) d\tau \right]. \end{aligned} \quad (40)$$

This expression is used as a radiation condition \mathbf{Z}_{ray} at the end of the finite length duct.

A. Resonance wavenumbers for the planar mode without influence of higher order duct modes

In a first instance, we consider the resonance wavenumbers of the planar mode ($m=n=0$) without the influence of higher order duct modes ($l=0$). With radiation, the j^{th} resonance wavenumbers of mode mn are denoted $k_{mn,r}^j$ and denoted k_{mn}^j without radiation.

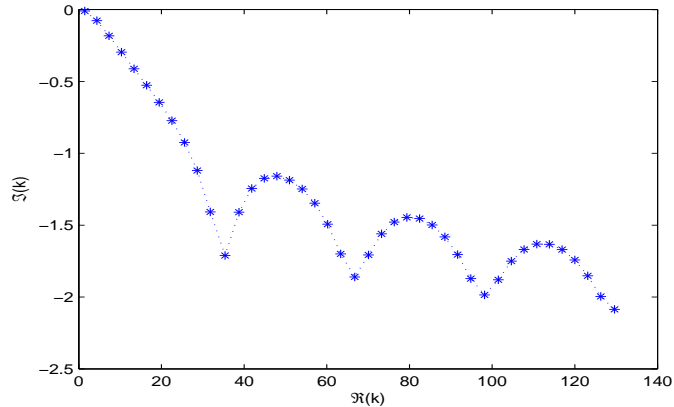


FIG. 4. Evolution of resonance wavenumbers $k_{00,r}^j$ depending on wave number k (for $b = 0.1m$ and $L = 1m$) for $m = n = 0$ and $l = 0$.

It is worth noting in Table I of Appendix B that without radiation, the resonance frequencies are those obtained by the usual longitudinal resonances of a cylindrical duct with one side "closed" and the other side "open" (Neumann/Dirichlet problem) for:

$$k_{00}^j = \frac{(2j+1)\pi}{2L}, j = 0, 1, 2, \dots$$

We can observe in Table I of Appendix B that the real part of resonance frequency decreases when radiation is taken into account: this is normal behavior because the reactive effect of radiation can roughly be described as an increase in the duct length. The semi-infinite duct length correction is estimated by the following formula (see Ref. 10 with the modification

given in private communication):

$$\frac{\Delta L}{b} = 0.82159 \frac{1 + \frac{kb}{1.2949}}{1 + \frac{kb}{1.2949} + \left(\frac{kb}{1.2949}\right)^2}. \quad (41)$$

Figure 5 shows that the difference between the real part of the first resonance frequency $k_{00,r}^0$ of a finite radiating cylindrical duct and that estimated using the length correction defined by Eq. (41) ($k_{00,\Delta L}^j = (2j + 1)\pi/[2(L + \Delta L)]$), tends to zero when the ratio L/b increases. The values agree well ($\leq 1\%$ of difference) for $L/b \geq 2$ with several values of L , when dissipative effects are low.

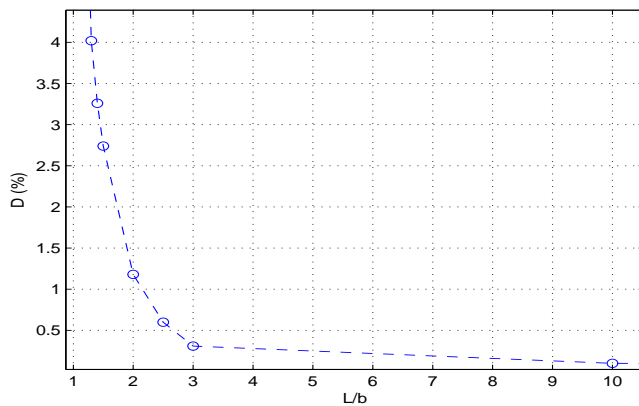


FIG. 5. Absolute value of difference in percent ($D = \frac{|\Re(k_{00,r}^0) - k_{00,\Delta L}^j|}{\Re(k_{00,r}^0)} * 100$) between the value of the real part of the first resonance wavenumber calculated by Newton's method ($k_{00,r}^0$) and that estimated with the length correction defined by the Eq. (41) ($k_{00,\Delta L}^j$), for several ratios L/b .

B. Resonance wavenumbers with influence of higher order duct modes

The principal interest of the complex Zorumski's formulation is that we can observe the influence of higher order duct modes (also denoted by H.M afterward). In this paper, we taken into account only the axisymmetric modes ($m = 0$). Figure 6 shows resonance wavenumbers $k_{00,r}^j$, $k_{01,r}^j$, $k_{02,r}^j$. We observe three series of resonances. Each series starts at

the cutoff frequency of a duct mode. The first one corresponds to a domination of the planar duct mode, the second to a domination of mode 01 and the third to a domination of mode 02 (see Appendix D). Fig. 7 shows the influence of the two first higher order duct modes ($m = 0, l = 1$ and $m = 0, l = 2$) on the resonance wavenumbers of the first series. It is worth noting that below the first cut off wavenumber $k_{cut01} = 3.83/b$, only one higher order duct mode is sufficient to accurately describe the resonances; between the first and second cut off wavenumber only two higher order duct modes are enough and similarly to the higher order duct modes: between the n^{th} and $(n + 1)^{th}$ cut off, only $(n + 1)$ higher order duct modes are enough.

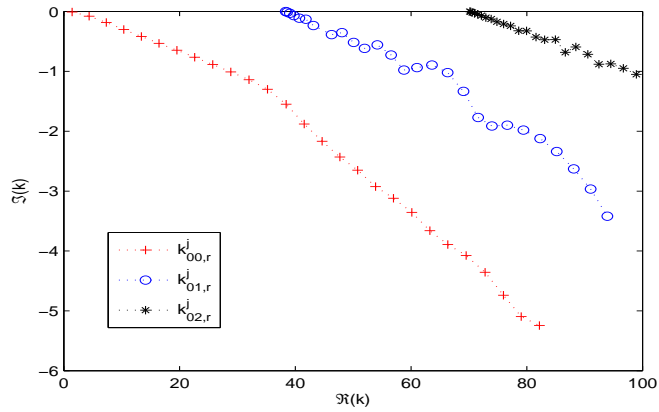


FIG. 6. Resonance wavenumbers $k_{00,r}^j$, $k_{01,r}^j$, $k_{02,r}^j$ for $L = 1m$ and $b = 0.1m$

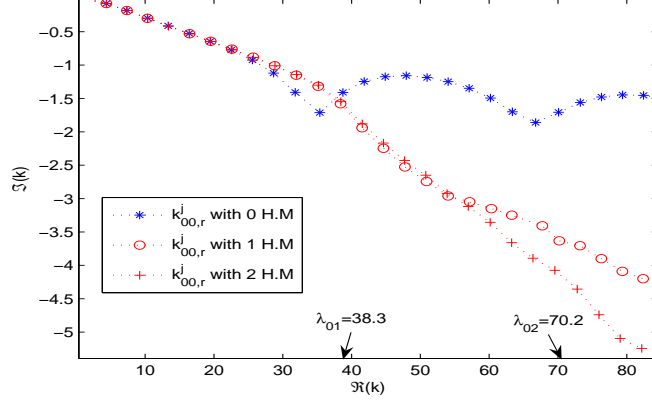


FIG. 7. Resonance wavenumbers $k_{00,r}^j$ of the first series ($m = 0, n = 0$) with an influence of 0 ($l = 0$), 1 ($l = 1$) and 2 ($l = 2$) H.M for $L = 1m$ and $b = 0.1m$

C. Evolution of the j first resonance wavenumbers with respect to radiation

In the present section, we show the evolution of the j first resonance wavenumbers when only the planar duct mode propagates with respect to radiation and as shown in the previous section, we take into account the effect of one higher order duct mode. For this purpose, we introduce a multiplicative coefficient on the radiation impedance. Physically, this coefficient η_ρ can be regarded as the ratio between the external fluid density ρ_{ext} and the internal fluid density ρ_{int} , such as:

$$\eta_\rho = \frac{\rho_{ext}}{\rho_{int}}, \quad (42)$$

the density of the external fluid ρ_{ext} varying from a vacuum to water density, the sound celerity, $340m.s^{-1}$, remaining constant.

Figures 8 and 9 show that when the parameter η_ρ increases, a Neumann/Neumann problem is obtained: the real part tends to $j\pi/L$ and the imaginary part tends to zero. This behavior corresponds to a system without losses, the external fluid becoming a perfectly reflective surface (to facilitate reading, η_ρ is denoted X and $\Re(k_{00,r}^j)$ is denoted Y within the figures).

Fig. 9 shows that the absolute value of the imaginary part of the resonance frequency

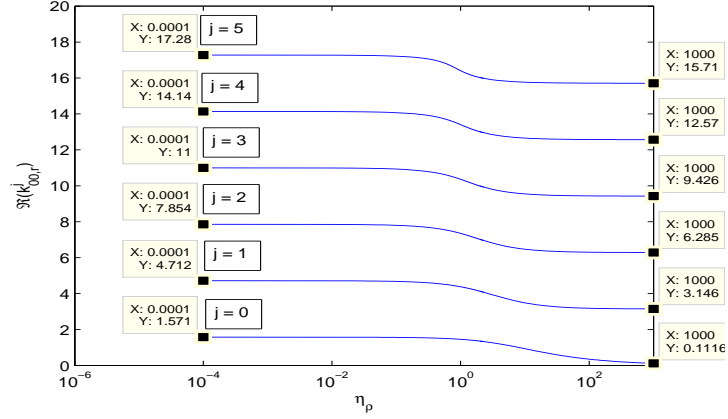


FIG. 8. Evolution of the real part of the j first longitudinal resonance wavenumbers $k_{00,r}^j$ with respect to η_ρ , for $L = 1m$ and $b = 0.1m$.

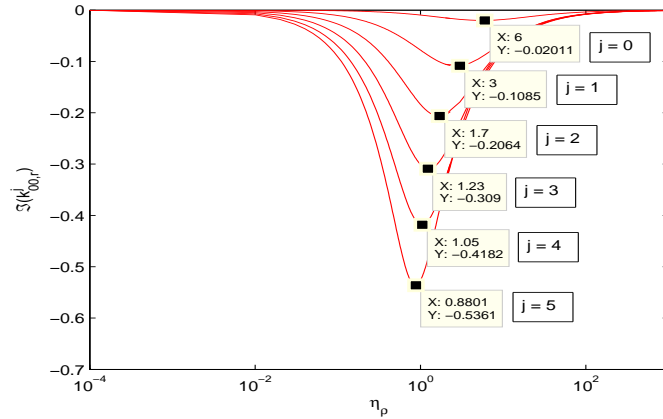


FIG. 9. Evolution of the imaginary part of the j first longitudinal resonance wavenumbers $k_{00,r}^j$ with respect to η_ρ , for $L = 1m$ and $b = 0.1m$; the dark square shows the maximum of $\Im(k_{00,r}^j)$.

goes through a maximum (showed by a dark square in each curve), corresponding to the maximum of the radiation. The physical case (for the problem under consideration) corresponds to $\eta_\rho = 1$, the same fluid inside and outside the duct. Thus, it can be interesting to study the evolution of resonances in this case for several values of the ratio b/L .

D. Evolution of the two first resonance frequencies of the planar mode for several ratios b/L

For this study, we introduce the loss factor ζ_{mn}^j describing the ratio between the imaginary part and real part of the resonance frequency: $\zeta_{mn}^j = \frac{\Re(k_{mn,r}^j)}{|\Im(k_{mn,r}^j)|}$. Figures 10 and 11 show that the loss factor increases with radius and decreases with length. Therefore, it can be concluded that radiation energy losses increase with radius and decrease with length. Moreover, we can observe that if ratio $b/L < 1$, only one higher order duct mode is sufficient to describe the resonances.

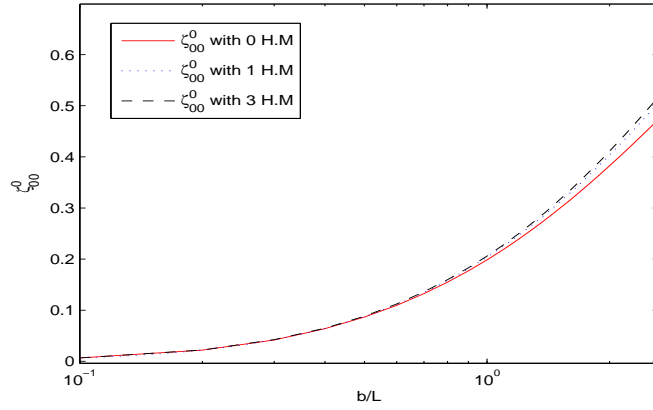


FIG. 10. Loss factor ζ_{00}^0 of the first resonance frequency of the planar mode with respect to ratio b/L

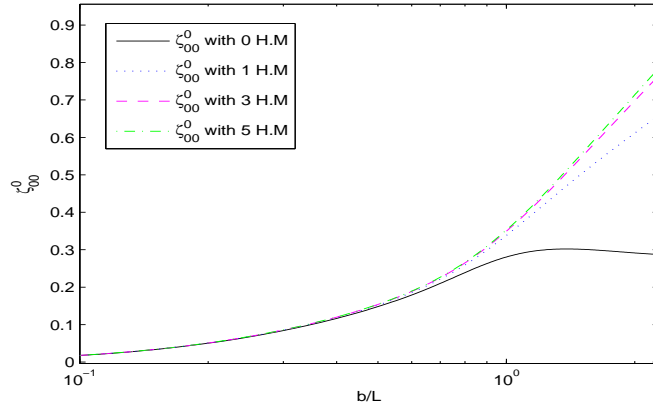


FIG. 11. Loss factor ζ_{00}^1 of the second resonance frequency of the planar mode with respect to ratio b/L

V. CONCLUSION

A development of the Green's function for the Helmholtz equation in a free space valid for complex frequencies is possible and leads to a new formula in Zorumski's radiation impedance. The interest has been shown for an application example, dedicated to the calculations of the complex resonances frequencies of a radiating flanged cylindrical duct. It has been shown that length correction calculated for a semi-infinite duct is a good estimate of a finite duct radiation when the ratio $L/b \geq 2$ and for frequencies sufficiently below the first cut off frequency. The study of the relation between radiation and several parameters is shown to be a way to optimize geometry for minimizing (e.g. for noise pollution) or maximizing the sound radiation (e.g. for wind instruments). The study of the influence of higher order duct modes has shown that below the first cut off frequency, only one higher order duct mode is needed to accurately describe the influence of the external fluid on the resonances and between the n^{th} and $(n + 1)^{th}$ cut off, only $(n + 1)$ higher order duct modes are enough. In the future, it will be interesting to use a BEM method to study more complicated geometries and to observe the resonances with an experimental method.

Acknowledgments

The authors wish to thank P. Herzog and F. Silva for their useful discussion points.

APPENDIX A: MATRICIAL CALCULATION

The main steps required to obtain the results are presented (see Ref. 17).

For a cylinder, the general solutions at point z_1 can be described with respect to the values of P and V at point z_2 such as described by relation (24). For all the modes mn , the following matrix problem is obtained:

$$\mathbf{P}(z_1) = \mathbf{C}\mathbf{P}(z_2) + \mathbf{Z}_c\mathbf{S}\mathbf{V}(z_2), \quad (\text{A1})$$

$$\mathbf{V}(z_1) = \mathbf{Z}_c^{-1}\mathbf{S}\mathbf{P}(z_2) + \mathbf{C}\mathbf{V}(z_2), \quad (\text{A2})$$

\mathbf{C} being a diagonal matrix constituted by the elements $\cosh(ik_{mn}(z_2 - z_1))$ et \mathbf{S} a diagonal matrix constituted by the elements $\sinh(ik_{mn}(z_2 - z_1))$. Eq. (A2) implies:

$$\mathbf{P}(z_2) = \mathbf{Z}_c\mathbf{S}^{-1}\mathbf{V}(z_1) - \mathbf{Z}_c\mathbf{S}^{-1}\mathbf{C}\mathbf{V}(z_2). \quad (\text{A3})$$

Introducing Eq. (A3) in Eq. (A1) and using the commutativity of the diagonal matrices, we obtain:

$$\mathbf{P}(z_1) = \mathbf{Z}_c\mathbf{S}^{-1}\mathbf{C}\mathbf{V}(z_1) - [\mathbf{Z}_c\mathbf{S}^{-1}\mathbf{C}\mathbf{C} - \mathbf{Z}_c\mathbf{S}]\mathbf{V}(z_2),$$

with

$$\begin{aligned} \mathbf{Z}_c\mathbf{S}^{-1}\mathbf{C}\mathbf{C} - \mathbf{Z}_c\mathbf{S} &= \mathbf{Z}_c\mathbf{S}^{-1}(\mathbf{I} + \mathbf{S}\mathbf{S}) - \mathbf{Z}_c\mathbf{S} \\ &= \mathbf{Z}_c\mathbf{S}^{-1} + \mathbf{Z}_c\mathbf{S} - \mathbf{Z}_c\mathbf{S} \\ &= \mathbf{Z}_c\mathbf{S}^{-1}, \end{aligned}$$

thus:

$$\mathbf{P}(z_1) = \mathbf{Z}_c\mathbf{S}^{-1}\mathbf{C}\mathbf{V}(z_1) - \mathbf{Z}_c\mathbf{S}^{-1}\mathbf{V}(z_2). \quad (\text{A4})$$

Therefore, with Eqs. (A3) and (A4), we obtain the relation (26).

APPENDIX B: NUMERICAL VALUES

The numerical values of the j first resonance wavenumbers without radiation (k_{00}^j) and with radiation ($k_{00,r}^j$) are represented here (with $b = 0.1m$ and $L = 1m$) in table I.

APPENDIX C: COMPARISON OF EXACT RESULTS WITH LOW FREQUENCY APPROXIMATION

In order to validate the complex formulation of the radiation impedance, we compare the resonances obtained with radiation impedance given by relation (40) for $m = n = 0$ and $l = 0$, with the resonances obtained with the radiation impedance of a flanged plane piston given by Rayleigh's formulation as (see Ref. 14 p.1458):

$$Z_0 \simeq \rho c \left[1 - \frac{1}{kb} J_1(2kb) - \frac{i}{kb} S_1(2kb) \right] \quad (C1)$$

The radiation impedance for $m=n=l=0$ calculated with relation (40) and that of a flanged plane piston are similar. Thus, resonance wavenumbers calculated with the radiation impedance Z_{000} obtained with the complex Zorumski's formulation (40) and with Rayleigh's formulation (C1) are identical, as observed in Fig. 12.

Figure 12 shows that resonance wavenumbers calculated with the radiation impedance Z_{000} obtained with the complex Zorumski's formulation (40) and with Rayleigh's formulation (C1) are identical, thus it confirms that these two formulations of radiation impedance are very similar.

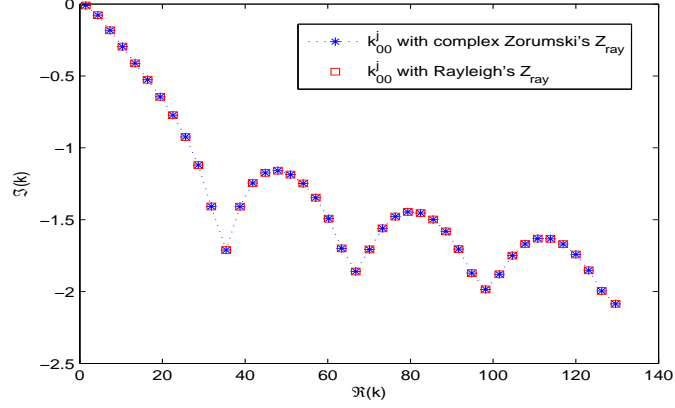


FIG. 12. Evolution of resonance wavenumbers $k_{00,r}^j$ depending on wave number k (with $b = 0.1m$ and $L = 1m$) with the radiation impedance defined by Eq. (40) for $m = n = 0$ and $l = 0$ (*) and with the radiation impedance of a flanged plane piston (Eq. C1) (\square).

APPENDIX D: GREEN'S FUNCTION PROFILE IN THE DUCT AROUND RESONANCE FREQUENCIES

Figures 13 and 14 show that around the resonance frequency k_{00}^{14} , the profile of Green's function corresponds to the profile of the planar mode even if mode 01 is propagating. The same comportment is observed around other resonance frequencies. Therefore, it is worth noting that each series observed in Fig. 6 corresponds to a predominant duct mode even if other modes are propagating.

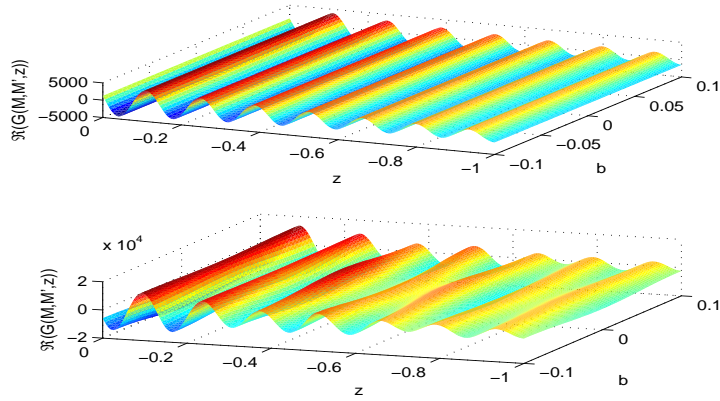


FIG. 13. Profile in the duct of the real part of Green's function of k_{00}^{14} with 0 H.M (upper figure) and 3 H.M (lower figure)

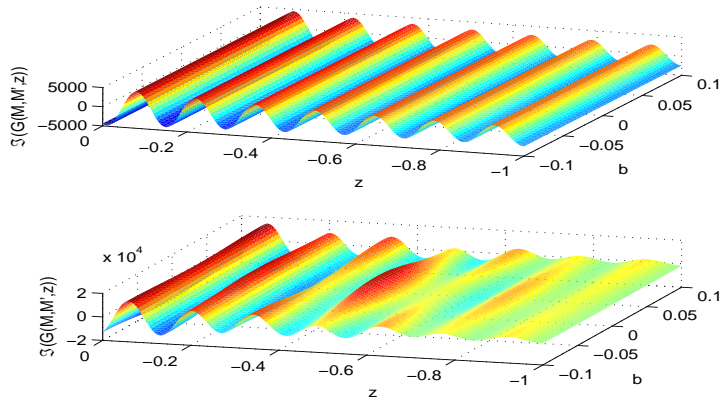


FIG. 14. Profile in the duct of the imaginary part of Green's function of k_{00}^{14} with 0 H.M (upper figure) and 3 H.M (lower figure)

REFERENCES

- ¹ L. Rayleigh, *The Theory of Sound (volume 2)* (Dover, New York) (1945).
- ² W. Zorumski, "Generalized radiation impedances and reflection coefficients of circular and annular ducts", *J. Acoust. Soc. Am.* **54**, 1667–1673 (1973).
- ³ G. Watson, *A Treatise on the Theory of Bessel Functions* (Cambridge U. P.) (1962).

- ⁴ W. Shao and C. Mechefske, “Analyses of radiation impedances of finite cylindrical ducts”, *Journal of Sound and Vibration* **286**, 363–381 (2005).
- ⁵ A. Kuijpers, S. Rienstra, G. Verbeek, and J. Verheij, “The acoustic radiation of baffled finite ducts with vibrating walls”, *Journal of Sound and Vibration* **216**, 461–493 (1998).
- ⁶ V. Pagneux, N. Amir, and J. Kergomard, “A study of wave propagation in varying cross-section waveguides by modal decomposition. part ii. results”, *J. Acoust. Soc. Am.* **101**, 2504–2517 (1997).
- ⁷ N. Amir and H. Matzner, “The acoustics of flanged cylindrical pipe, examining the influence of higher order modes”, *Acustica* **90**, 1–7 (2004).
- ⁸ L. Campos and J. Oliveira, “On the acoustic modes in a cylindrical duct with an arbitrary wall impedance distribution”, *J. Acoust. Soc. Am.* **116**, 3336–3347 (2004).
- ⁹ W. Zorumski and J. Mason, “Multiple eigenvalues of sound-absorbing circular and annular ducts”, *J. Acoust. Soc. Am.* **55**, 1158–1165 (1974).
- ¹⁰ A. Norris and I. Sheng, “Acoustic radiation from a circular pipe with an infinite flange”, *Journal of Sound and Vibration* **135**, 85–93 (1989).
- ¹¹ Y. Nomura, I. Yamamura, and S. Inawashiro, “On the acoustic radiation from a flanged circular pipe”, *Journal of the Physical Society of Japan* **15**, 510–517 (1960).
- ¹² H. Levine and J. Schwinger, “On the radiation of sound from an unflanged circular pipe”, *Physical Review* .
- ¹³ M. Abramowitz and I. A. Stegun, *Handbook of Mathematical Functions* (Dover, New York) (1968).
- ¹⁴ M. Morse and H. Feshbach, *Methods of Theoretical Physics (Part I)* (McGraw-Hill, New York) (1953).
- ¹⁵ F. Silva, P. Guillemain, J. Kergomard, B. Mallaroni, and A. N. Norris, “Approximation formulae for the acoustic radiation impedance of a cylindrical pipe”, submitted to *Journal of Sound and Vibration* (2008).
- ¹⁶ V. Pagneux, N. Amir, and J. Kergomard, “A study of wave propagation in varying cross-section waveguides by modal decomposition. part i. theory and validation”, *J. Acoust.*

Soc. Am. **100**, 2034–2048 (1996).

- ¹⁷ J. Kergomard, “Calculation of discontinuities in waveguides using mode-matching method: an alternative to the scattering matrix approach”, *J. Acoustique* **4**, 111–138 (1991).

j	k_{00}^j	$k_{00,r}^j$ with 0 H.M	$k_{00,r}^j$ with 1 H.M
0	1.5708	1.449 - 0.0095i	1.451 - 0.0096i
1	4.712	4.369-0.077i	4.375-0.0776i
2	7.854	7.333-0.182i	7.345-0.183i
3	10.996	10.336-0.296i	10.345-0.299i
4	14.137	13.365-0.412i	13.4-0.415i
5	17.279	16.409-0.526i	16.45-0.53i
6	20.42	19.463-0.645i	19.523-0.644i
7	23.562	22.523-0.773i	22.608-0.76i
8	26.7	25.59 -0.924i	25.707-0.881i
9	29.85	28.674-1.12i	28.824-1.01i
10	32.99	31.822-1.408i	31.965-1.152i
11	36.13	35.377-1.711i	35.149-1.317i
12	39.27	38.747-1.409i	38.395-1.579i

TABLE I. Values of the j first resonance wavenumbers without radiation (k_{00}^j) and with radiation ($k_{00,r}^j$) for 0 and 1 H.M, with $b = 0.1m$ and $L = 1m$, for $m = n = 0$.

LIST OF FIGURES

FIG. 1	Schema and coordinates of the duct.	4
FIG. 2	Deformation of the integration contour.	7
FIG. 3	Real part (solid curve) and absolute value of imaginary part (dashed curve) of the radiation impedance for the planar mode ($m = n = 0$ and $l = 0$) with respect to wavenumber k , calculated with Zorumski's formulation (7) (solid and dashed curves) and with modified formulation (17) (crosses).	9
FIG. 4	Evolution of resonance wavenumbers $k_{00,r}^j$ depending on wave number k (for $b = 0.1m$ and $L = 1m$) for $m = n = 0$ and $l = 0$	16
FIG. 5	Absolute value of difference in percent ($D = \frac{ \Re(k_{00,r}^0) - k_{00,\Delta L}^j }{\Re(k_{00,r}^0)} * 100$) between the value of the real part of the first resonance wavenumber calculated by Newton's method ($k_{00,r}^0$) and that estimated with the length correction defined by the Eq. (41) ($k_{00,\Delta L}^j$), for several ratios L/b	17
FIG. 6	Resonance wavenumbers $k_{00,r}^j, k_{01,r}^j, k_{02,r}^j$ for $L = 1m$ and $b = 0.1m$	18
FIG. 7	Resonance wavenumbers $k_{00,r}^j$ of the first series ($m = 0, n = 0$) with an influence of 0 ($l = 0$), 1 ($l = 1$) and 2 ($l = 2$) H.M for $L = 1m$ and $b = 0.1m$	19
FIG. 8	Evolution of the real part of the j first longitudinal resonance wavenumbers $k_{00,r}^j$ with respect to η_ρ , for $L = 1m$ and $b = 0.1m$	20
FIG. 9	Evolution of the imaginary part of the j first longitudinal resonance wavenumbers $k_{00,r}^j$ with respect to η_ρ , for $L = 1m$ and $b = 0.1m$; the dark square shows the maximum of $\Im(k_{00,r}^j)$	20
FIG. 10	Loss factor ζ_{00}^0 of the first resonance frequency of the planar mode with respect to ratio b/L	21
FIG. 11	Loss factor ζ_{00}^1 of the second resonance frequency of the planar mode with respect to ratio b/L	22

FIG. 12	Evolution of resonance wavenumbers $k_{00,r}^j$ depending on wave number k (with $b = 0.1m$ and $L = 1m$) with the radiation impedance defined by Eq. (40) for $m = n = 0$ and $l = 0$ (*) and with the radiation impedance of a flanged plane piston (Eq. C1) (\square).	25
FIG. 13	Profile in the duct of the real part of Green's function of k_{00}^{14} with 0 H.M (upper figure) and 3 H.M (lower figure)	26
FIG. 14	Profile in the duct of the imaginary part of Green's function of k_{00}^{14} with 0 H.M (upper figure) and 3 H.M (lower figure)	26